19

Mechanical Properties of Optical Fibers

Paulo Antunes, Fátima Domingues, Marco Granada and Paulo André
Instituto de Telecomunicações and Departamento de Física, Universidade de Aveiro
Portugal

1. Introduction

Nowadays, optical communications are the most requested and preferred telecommunication technology, due to its large bandwidth and low propagation attenuation, when compared with the electric transmission lines. Besides these advantages, the use of optical fibers often represents for the telecom operators a low implementation and operation cost.
Moreover, the applications of optical fibers goes beyond the optical communications topic. The use of optical fiber in sensors applications is growing, driven by the large research done in this area in recent years and taking the advantages of the optical technology when compared with the electronic solutions. However, the implementation of optical networks and sensing systems in seashore areas requires a novel study on the reliability of the optical fiber in such harsh environment, where moisture, Na^+ and Cl^- ions are predominant.
In this work we characterize the mechanical properties, like the elastic constant, the Young modulus and the mean strain limit for commercial optical fibers. The fiber mean rupture limit in standard and Boron co-doped photosensitive optical fibers, usually used in fiber Bragg grating based sensors, is also quantify. Finally, we studied the effect of seawater in the zero stress aging of coated optical fibers. Such values are extremely relevant, providing useful experimental values to be used in the design and modeling of optical sensors, and on the aging performance and mechanical reliability studies for optical fiber cables.

2. Mechanical properties

The optical fibers are mainly used as the transmission medium in optical communications systems, nevertheless its applications in sensing technology is growing. Although the optical fiber mechanical properties are important for its use in optical communications (bending radius) is on the sensing applications that these properties are more relevant. In sensing technology the physical properties of the optical fiber are essential for the sensors characterization. Most of the optical fiber based sensors rely on the deformation of the optical fiber to determine the external parameter of interest. As an example, fiber Bragg grating (FBG) are one of the most promising technologies in sensing applications due to it numerous advantages, like small size, reduced weight, low attenuations, immunity to electromagnetic interference and electrical isolation (Antunes et al., 2011). The FBG concept as sensor relies on the mechanical deformation of the optical fiber to measure static or dynamic parameters like deformation, temperature or acceleration, therefore it is crucial to know the mechanical properties of the optical fiber (Antunes et al., 2008).

If an optical fiber is perturbed mechanically, it will suffer a deformation proportional to the amplitude of the perturbation force. This approach is valid for perturbations values lower than the elastic limit of the optical fiber, where the mechanical perturbations are reversible.
The Hooke's law expresses the relation between the perturbation force and the produced deformation, the proportionality is given by the material elastic constant. The Hooke's law is given by the following expression, along the longitudinal axis of the fiber:

$$K = \frac{|F|}{|\Delta L|} \tag{1}$$

where K is the elastic constant and Δl is the relative deformation imposed by the action of the perturbation force, F.
The fiber Young modulus, E_G, is the proportionality constant between the perturbation force per area and the relative deformation:

$$F = E_G A \frac{\Delta l}{l} \tag{2}$$

In expression (2), A is area and l is length the optical fiber under perturbation. Considering expressions (1) and (2), the elastic constant is given by:

$$|K| = \frac{E_G A}{l} \tag{3}$$

According to expression (2), the slope of the linear region (elastic region) of the perturbation force as a function of the relative deformation represents the product $E_G \times A$. This product can be used in expression (3) to obtain the elastic constant of the optical fiber, knowing its length.
In this work we tested standard optical communications fiber SMF-28e from Corning, which according to the manufacturer specifications, have an uncoated diameter of 125.0±0.3 μm and 245±5 μm with the protective coating and photosensitive optical fiber PS1250/1500 co-doped fiber, from FiberCore, with 125±1 μm diameter without coating.
The strain measurements were made using a Shimadzu AGS-5kND mechanical test machine. The tested optical fibers were: ten samples of standard optical fiber with the acrilate protective coating; nine samples of standard optical fiber without the acrilate protective coating and ten samples of photosensitive optical fiber without the acrilate protective coating. Each sample had a length of 20.0 cm and was glued, with Cyanoacrylate glue, in each extremity to an aluminum plate to make it possible the fixation to the mechanical test machine.
Figure 1 shows photography of one optical fiber samples.

Fig. 1. Photography of a tested optical fiber with the glued aluminum plates on the extremities.

The experimental data collected with the mechanical test machine allows the representation of the force versus strain curves, for each sample of fiber.
Figure 2 shows the force versus strain graphic, representing the force applied along the fiber longitudinal axis, for each of the ten samples of standard optical fiber with the acrilate protective coating.

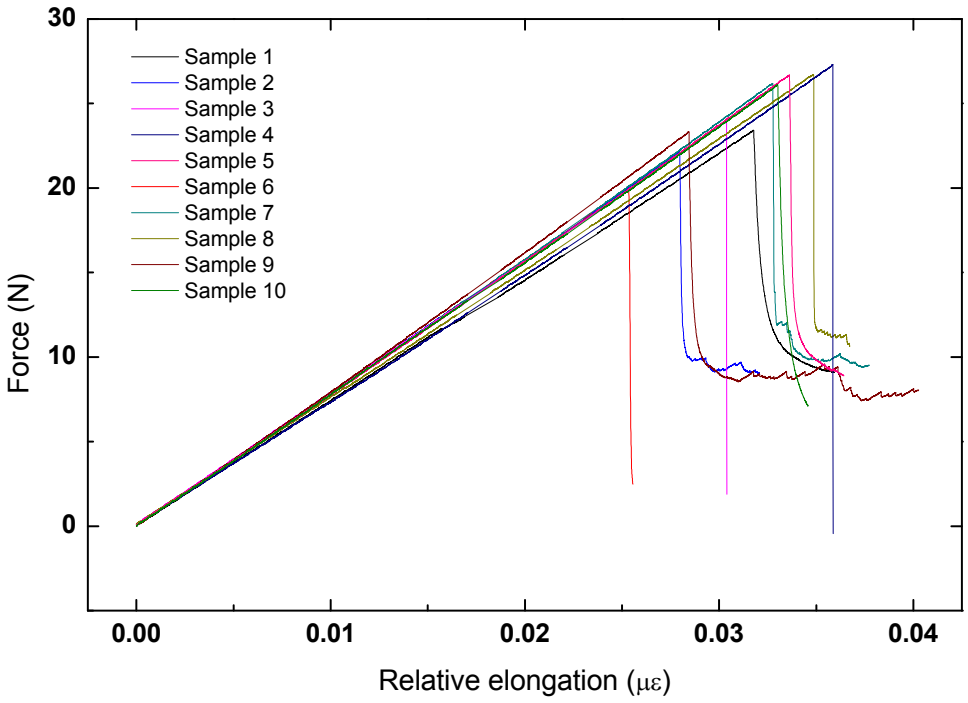

Fig. 2. Force versus strain experimental data for each sample of the standard optical fiber with the acrilate protective coating.

Considering the ten fiber samples of standard optical fiber with the acrilate protective coating, the average value for the product $E_G \times A$ is 780.87±24.99 N and the average rupture force value for the fibers fracture is 24.60±2.38 N.
The force versus strain curves for the standard fiber without the protective coating samples are presented in figure 3.
The average value obtained for the $E_G \times A$ product of the standard optical fiber without the coating was 849.42±6.88 N and the average rupture force was 4.35±1.45 N.
The force versus strain curve for the photosensitive optical fiber without the protective coating is presented in figure 4.

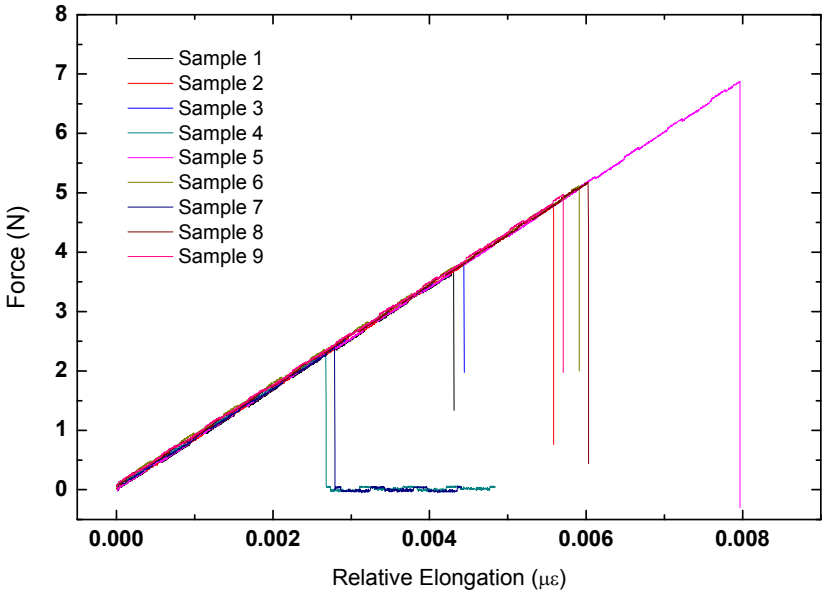

Fig. 3. Force versus strain experimental data for each sample of standard optical fiber without the acrilate protective coating.

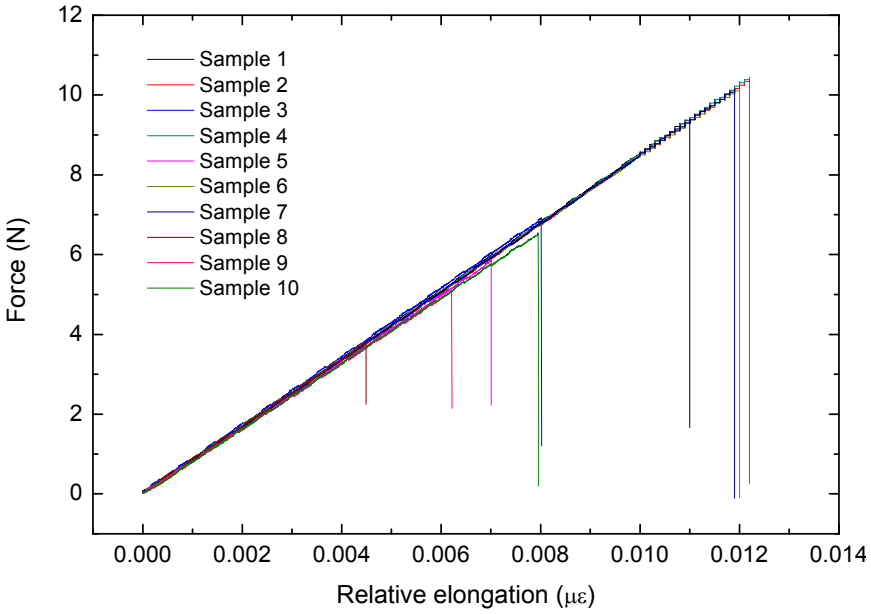

Fig. 4. Force versus strain experimental curve for the ten samples of photosensitive optical fiber without the acrilate protective coating.

For the photosensitive optical fiber without the coating the average value obtained for the $E_G \times A$ product was 841.30±15.06 N and the average rupture limit was 7.57±2.51 N.
Considering the area of each optical fiber type, the Young modulus can be obtained through the $E_G \times A$ product. The Young modulus for each type of optical fiber is presented in table 1, considering the average value of the $E_G \times A$ product.

Fiber	E_G *(GPa)*
Standard fiber with coating	16.56±0.39
Standard fiber without coating	69.22±0.42
Photosensitive fiber without coating	68.56±1.47

Table 1. Young modulus for different types of optical fiber.

The Young modulus values found in literature (Pigeon et al., 1992; Mita et al., 2000; Antunes et al., 2008) for silica and silica fibers are consistent with the ones we measure. The obtained values can be used in the design and modeling of optical fiber sensors were the fiber can be under some kind of stress, like FBG based sensors.

3. Optical fiber degradation behavior

The application of optical fiber in aggressive environments may lead to the degradation of its physic reliability and therefore the performance of the systems in which it is applied (El Abdi et al., 2010). Therefore, the conservation of the optical fiber physical characteristics in harsh environments, where the fiber is exposed to abrasion and moisture, is a key point to assure its good performance.
The optical fiber coatings can provide a robust protection from the extrinsic factors that may decrease its strength and performance. Nevertheless, and in spite of the protection provided by the coatings, the fiber is still permeable to moisture. There are reports of its ability to retain the hydroxyl groups from the water molecules,(Berger et al., 2003; Méndez et al., 2007; El Abdi et al., 2010; André et al., 2011), but also of the diffusion of other ions in addition to the ones from water. Such ions diffusion can be responsible for the optical fiber degradation and the decrease of its strength (Thirtha et al., 2002; Lindholm et al., 2004). Therefore, the behavior of the fiber strength with aging is not only dependent on the moisture present in the environment but also on the diffusion rate of the ions across the coating (Armstrong et al., 1999; Domingues et al., 2010).
The implementation of optical fiber systems (as for example in sensing structures or optical networks) (Ferreira et al., 2009), is dependent on the optical fiber reliability and its lifetime degradation in abrasive environments, where ions like Na+, Cl-, or even moisture are present.

3.1 Effect of maritime environment in the zero stress aging of optical fiber

To study the effect of maritime environment in the aging of optical fiber, several samples of a standard single mode fiber (SMF-28eR) fiber, manufactured by Corning, were left in a Sodium Chloride (NaCl) aqueous solution. The fiber under test had a diameter of 125 μm, d_f, and a total diameter of 250 μm with the coating, d_c. The effect of different NaCl concentrations were studied, namely, 0 (pure deionized water), 35, 100 and 250 g/L. The 35 g/L solution matches the average sea water concentration of NaCl, while the 250 g/L

corresponds to the highest Sodium Chloride concentration found in the Earth, namely in the Dead Sea.
During the tests, samples were removed from the NaCl solution and its fracture stress was measured. For that procedure it was used an experimental setup like the one represented in figure 5.

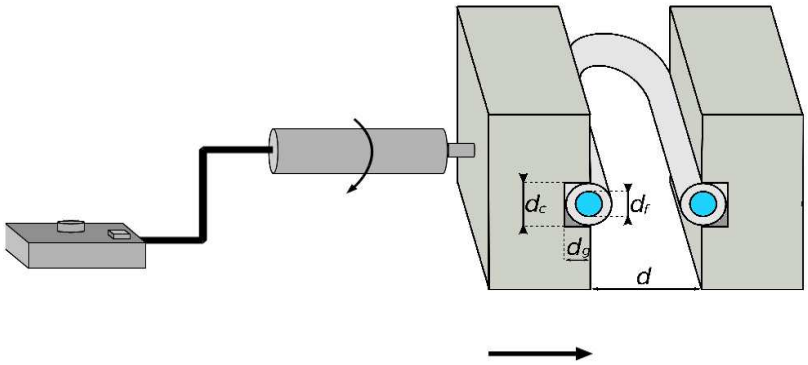

Fig. 5. Illustration of the experimental setup used to measure the fiber fracture stress.

The experimental setup uses a fixe PTFE plate and a moveable PTFE plate with grooves for the fiber fixing. The moveable plate is controlled by an electric translation stage (Newport, model 861). Initially, the plates have a distance between them of 20 mm. This distance is reduced at a speed of 0.55 mm/s. After the fiber break, the distance between plates is measured and related with the fiber fracture stress, which is dependent of the distance between the two plates. The stress applied in the fiber can be calculated through the equation (4)(El Abdi et al., 2010):

$$\sigma = E_0 \varepsilon \left(1 + \frac{1}{2} \alpha \varepsilon \right) \tag{4}$$

where σ is the stress in the fiber, E_0 the fiber young modulus, ε the strain in the fiber and α is a non linearity elastic parameter. The strain ε is given by (5):

$$\varepsilon = 1.198 \left[\frac{d_f}{d - d_c + 2d_g} \right] \tag{5}$$

where d_f is fiber diameter without the coating, d the distance between plates, d_c the fiber diameter with coating and d_g is the total depth of the two grooves. The non linearity elastic parameter, α, is given by:

$$\alpha = \frac{3}{4} \alpha' + \frac{1}{4} \tag{6}$$

For an optical fiber α'=6 (El Abdi et al., 2010). By applying equation (4) to the measured data, we can determinate the applied stress at which the fiber fractures. This procedure was executed for the NaCl concentrations previously referred and for different aging periods.

For every sample the average stress values and error were calculated for five identical samples. In figure 6 is presented the results obtained along the aging time for the three concentrations under study.

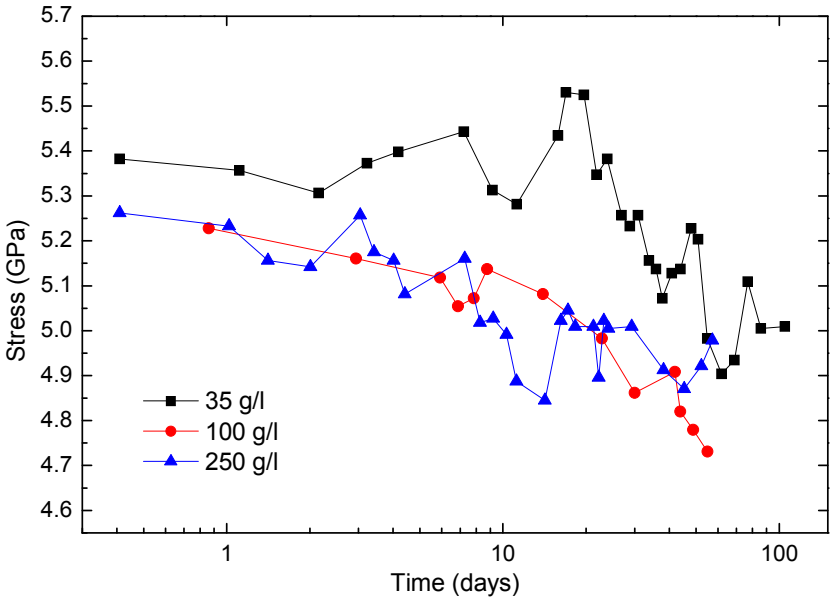

Fig. 6. Fracture stress values along degradation time for the fibers aged in the 35, 100 and 250 g/L NaCl solutions.

Several studies have reported that when the optical fiber is submitted to harsh environments its strength drastically drops after a certain time, showing a fatigue transition generally called as "knee". This behavior represents the sudden decrease of the optical fiber strength and the transition of its strength to a degradation regime (Armstrong et al., 1999; El Abdi et al., 2010). From the analyses of data collected is possible to observe that, for the fibers aged in the solutions with higher NaCl concentrations the strength of the fiber decreases and the "Knee" appears sooner in time.

In order to understand the stress behavior of aged fibers, the fracture stress values obtained for the three concentrations under study were fitted to a Boltzmann function, given by equation (7):

$$y = \frac{(A_1 - A_2)}{1 + \exp((x - x_0)/d_x)} + A_2 \tag{7}$$

The parameters A1 and A2 are the upper and lower limit of the fiber stress, respectively, x_0 is the activation parameter. The d_x parameter represents the function higher slope and assumes, in that point, a value of $(A2-A1)/(4d_x)$.

In figure 7 is presented the behavior of the fracture stress of the fiber as function of the exposition time in a logarithmic scale to the 35, 100 and 250 g/L NaCl concentrated solutions and the fit to the Boltzmann function:

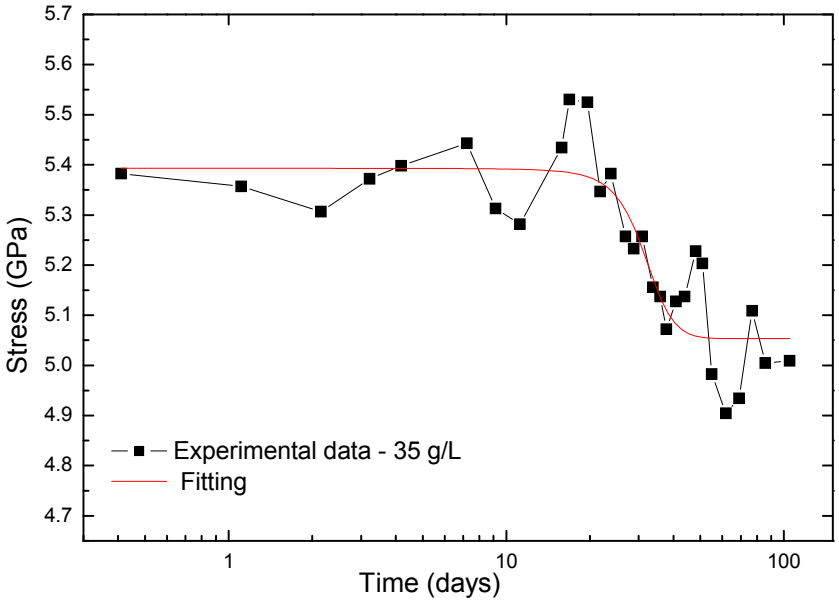
Stress (GPa)
Time (days)
Experimental data - 35 g/L
Fitting
5.7
5.6
5.5
5.4
5.3
5.2
5.1
5.0
4.9
4.8
4.7
1
10
100

a)

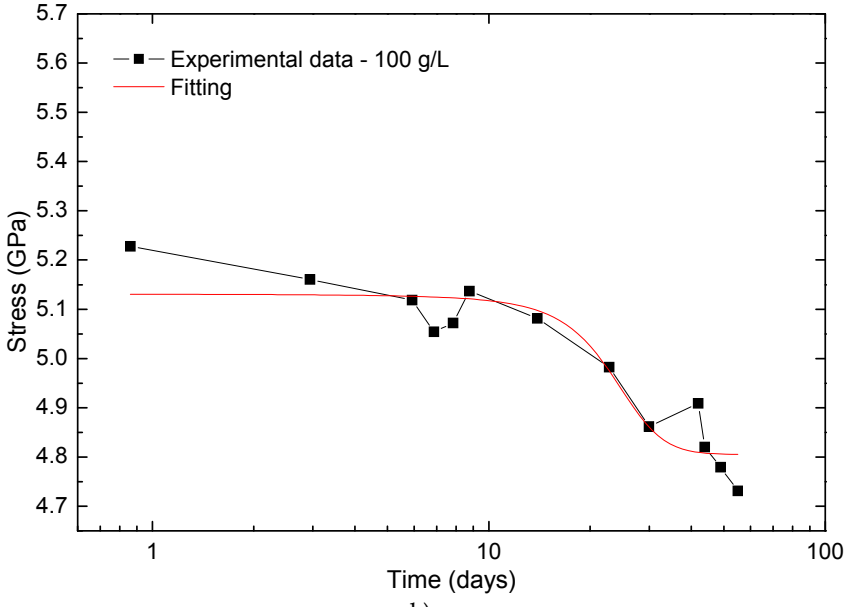
Stress (GPa)
Time (days)
Experimental data - 100 g/L
Fitting
5.7
5.6
5.5
5.4
5.3
5.2
5.1
5.0
4.9
4.8
4.7
1
10
100

b)

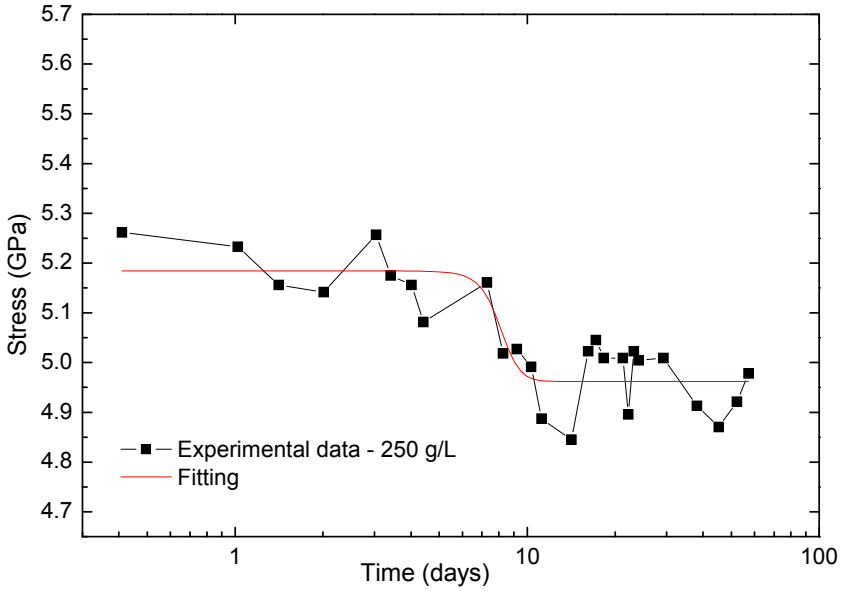

c)

Fig. 7. Fracture stress along time for the fibers aged in the a) 35, b) 100 and c) 250 g/L NaCl solutions and fitting to the Boltzmann function.

The table 2 displays the Boltzmann fit parameters for the three different concentrations.

Concentration (g/L)	A1 (GPa)	A2 (GPa)	x0 (days)	dx ($days^{-1}$)
35	5.39	5.05	31.34	3.97
100	5.13	4.80	23.13	4.30
250	5.18	4.96	8.05	0.65

Table 2. Boltzmann function fitting parameters.

From the values in table 2 we can see that, the time at which the strength transition occur (x_0) decreases with the increase of the NaCl concentration. If we establish a relation between the x0 value and the time at which the "knee" appears, we can affirm that the "Knee" will show up earlier for higher concentrations of NaCl.

This connection between the NaCl concentration and the time at which the strength transition occurs, is related to the ability of the ions in solution to infiltrate the fiber coating, react with the fiber glass surface, and remove the products through the coating (Thirtha et al., 2002). So, we can say that the diffusion through the coating of the species in solution or present in the environment in which the fiber is placed, has a major role on the aging behavior of the fiber, once such diffusion implies the decrease of the fiber strength and as consequence the decrease of its lifetime. In the analysis of the strength transition parameter, figure 8, we verify that the strength transition period has a degradation rate of 0.1174 days/[NaCl].

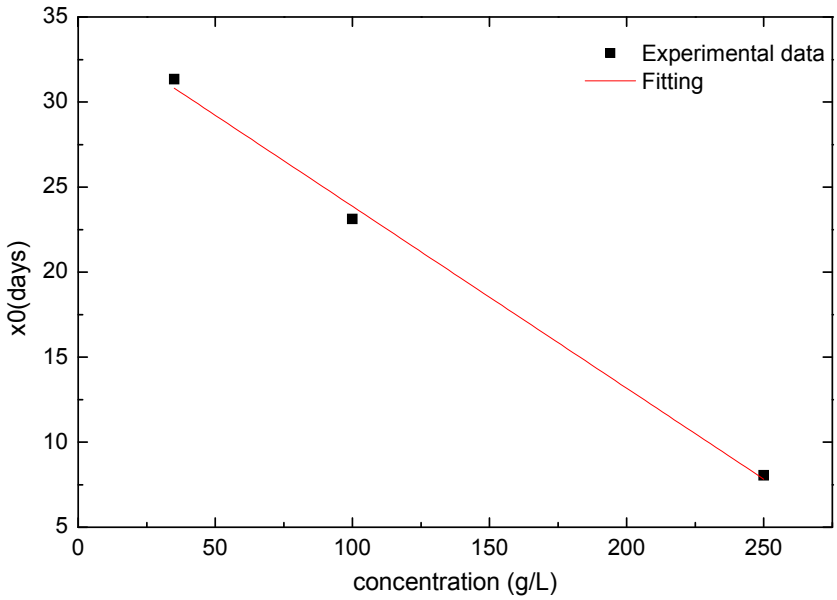

Fig. 8. Degradation rate of the aged optical fiber.

According to the authors (Danzer et al., 2007), the probability of fracture in a material increases with the number of flaws and with its dimension. Based on such assumption, the study of the probability to failure of the different aged samples will give us the information regarding the number of flaws in the samples.
To implement this study it was used the statistical Weibull's law given by:

$$\ln\left[\ln\left\{\frac{1}{1-F}\right\}\right] = m\left[\ln(\sigma) - \ln(\sigma_0)\right] \tag{8}$$

This law establishes the relation between the probability of fiber failure, F, with the applied stress σ. The first term represents the cumulative failure probability, and its evolution with the increase of the failure stress, ln(σ). The parameters σ_0 and m are constant, being m also referred to as the Weibull slope.
In the figure 9 it is represented the cumulative failure probability for fibers with no degradation and the ones aged in a 35 g/L solution of NaCl for 20 and 86 days.
It is possible to observe that the higher the aging period, the lower is the stress necessary to fracture the fiber.
Also for the different concentrations used and for the same aging periods, figure 10, it is clear that the higher the concentration of NaCl, the lower is the stress need for fracture to occur.

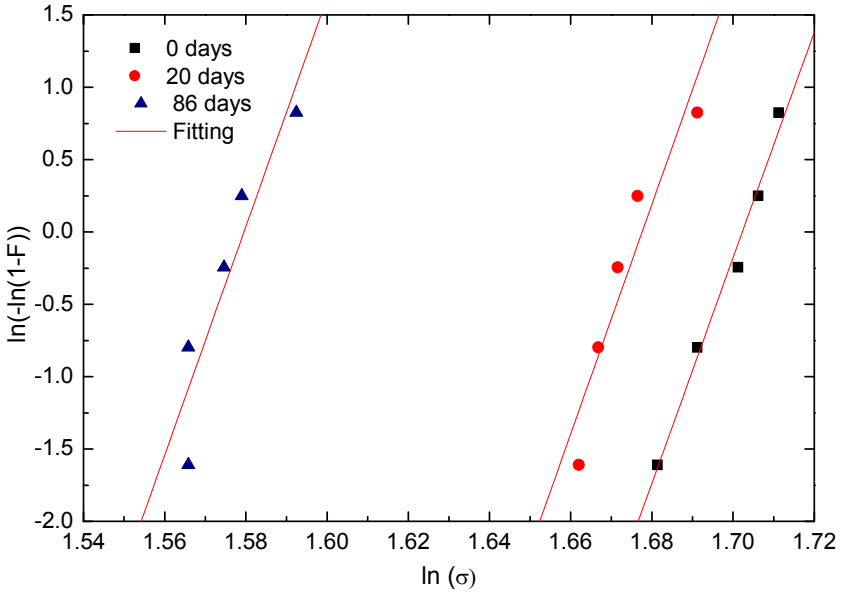

Fig. 9. Cumulative failure probability for fibers aged in the same NaCl concentration for different periods of time.

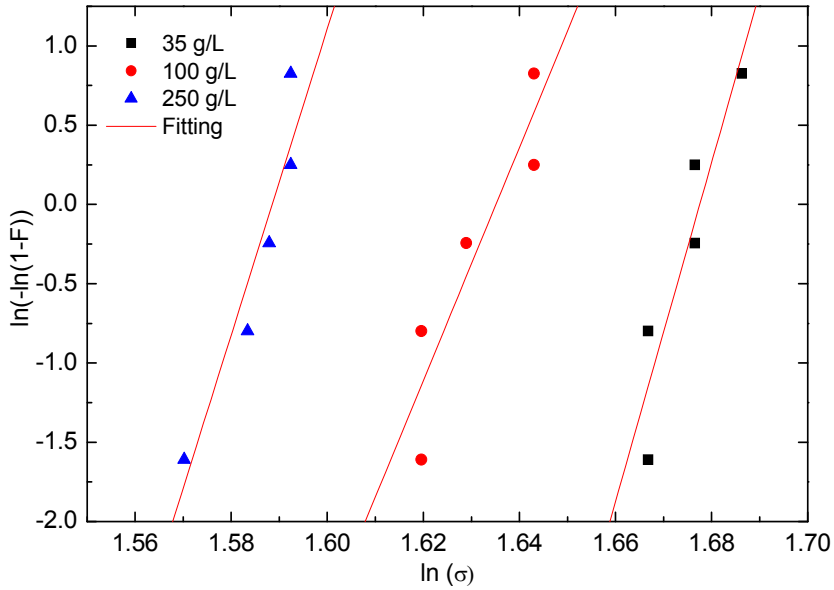

Fig. 10. Cumulative failure probability for fibers aged in different NaCl concentrations for the same period of time.

Through these latest analysis we may assume that the number of flaws in the fiber increases with the aging time and with the concentration of NaCl ions in solution.

3.2 Microscopic analysis of the aged optical fiber

In addition to the analytical study of the fibers, also its microscopic condition was analyzed through optical microscopy and SEM images.
In figure 11 we present the optical microscopy images, taken with an Olympus BH2 and the digital camera Sony DKC-CM30, for fibers degraded on a 35 g/l NaCl aqueous solution a) during 31 days and b) 105 days (Domingues et al., 2010).

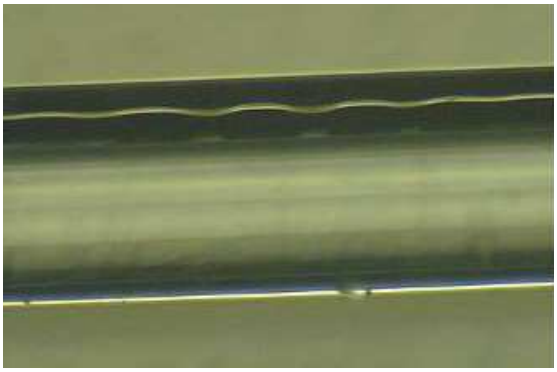

a)

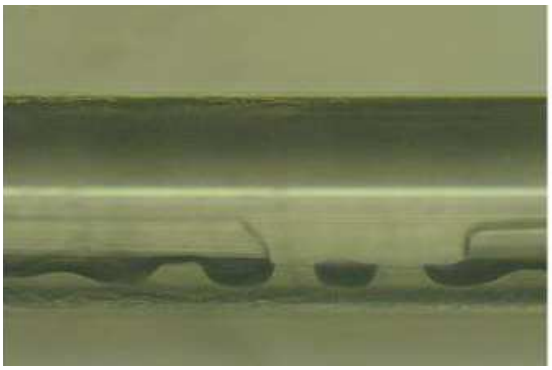

b)

Fig. 11. Microscopy images from fibers aged in a 35 g/l NaCl aqueous solution a) during 31 days and b) 105 days.

In these images we can see the difference in the protective polymer as consequence of its degradation.

The SEM images were obtained with an Hitachi SU-70 apparatus after carbon evaporation. In figure 12, are represented some of the images collected, for the three concentrations under study.

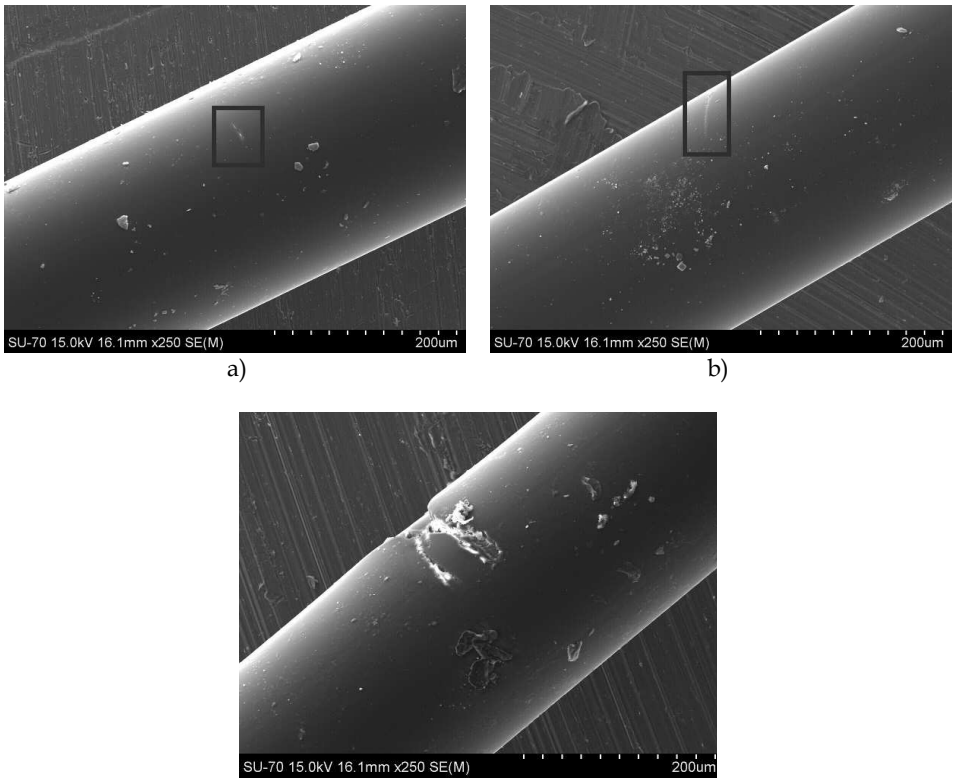

Fig. 12. SEM images from fibers aged in a) 35g/L NaCl solution for 105 days, b) 100g/L NaCl solution for 69 days and c) 250g/L NaCl solution for 64 days.

In these samples, it is possible to identify the damage induced in the coating in the three samples, being the most relevant, the one presented by the sample aged in a 250 g/L solution. But also in addition to the degradation, we can identify some NaCl crystal deposited in the fiber's surface.

4. Conclusions

We characterized the mechanical properties for commercial optical fibers. The Young modulus obtained has the value of 69.2 GPa for the standard optical fiber without the external acrilate protective coating. The effect of seawater in the zero stress aging of coated optical fiber, shows its increasing degradation with the Sodium Chloride concentration. The degradation rate has a value of 0.1174 days/[NaCl].

These results can be useful for the design and modeling of optical sensors, and on the aging performance of optical fiber deployed in telecommunication networks.

5. References

André, P. S., F. Domingues and M. Granada (2011). Impact of the Maritime Environment on the Aging of Optical Fibers, *Proceedings of CLEO2011: Laser Science to Photonic Applications*, Baltimore, USA.

Antunes, P., H. Lima, N. Alberto, L. Bilro, P. Pinto, A. Costa, H. Rodrigues, J. L. Pinto, R. Nogueira, H. Varum and P. S. André (2011). Optical sensors based on FBG for structural helth monitoring, in: *New Developments in Sensing Technology for Structural Health Monitoring*, S. C. Mukhopadhyay, Springer-Verlag.

Antunes, P., H. Lima, J. Monteiro and P. S. André (2008). Elastic constant measurement for standard and photosensitive single mode optical fibres, *Microwave and Optical Technology Letters*, Vol. 50, No. 9, pp. 2467-2469, ISSN: 1098-2760.

Armstrong, J. L., M. J. Matthewson, M. G. Juarez and C. Y. Chou (1999). The effect of diffusion rates in optical fiber polymer coatings on aging, *Optical Fiber Reliability and Testing*, Vol. 3848, pp. 62-69, ISSN: 0277-786X.

Berger, S. and M. Tomozawa (2003). Water diffusion into a silica glass optical fiber, *Journal of Non-Crystalline Solids*, Vol. 324, No. 3, pp. 256-263, ISSN: 0022-3093.

Danzer, R., P. Supancle, J. Pascual and T. Lube (2007). Fracture statistics of ceramics - Weibull statistics and deviations from Weibull statistics, *Engineering Fracture Mechanics*, Vol. 74, No. 18, pp. 2919-2932, ISSN: 0013-7944.

Domingues, F., P. André and M. Granada (2010). Optical Fibres Coating Aging induced by the Maritime Environment, *Proceedings of MOMAG2010*, Brasil.

El Abdi, R., A. D. Rujinski, M. Poulain and I. Severin (2010). Damage of Optical Fibers Under Wet Environments, *Experimental Mechanics*, Vol. 50, No. 8, pp. 1225-1234, ISSN: 0014-4851.

Ferreira, L. F., P. F. C. Antunes, F. Domingues, P. A. Silva, R. N. Nogueira, J. L. Pinto, P. S. Andre and J. Fortes (2009). Monitorization of Sea Sand Transport in Coastal Areas Using Optical Fiber Sensors, *2009 Ieee Sensors, Vols 1-3*, pp. 146-150

Lindholm, E. A., J. Li, A. Hokansson, B. Slyman and D. Burgess (2004). Aging behavior of optical fibers in aqueous environments, *Reliability of Optical Fiber Components, Devices, Systems, and Networks Ii*, Vol. 5465, pp. 25-32, ISSN: 0277-786X.

Méndez, A. and T. F. Morse (2007). *Specialty Optical Fibers Handbook*, Elsevier Inc.,

Mita, A. and I. Yokoi (2000). Fiber Bragg Grating Accelerometer for Structural Health Monitoring. Fifth International Conference on Motion and Vibration Control (MOVIC 2000). Sydney, Australia.

Pigeon, F., S. Pelissier, A. Mure-Ravaud, H. Gagnaire and C. Veillas (1992). Optical Fibre Young Modulus Measurement Using an Optical Method, *Electronics Letters*, Vol. 28, No. 11, pp. 1034-1035,

Thirtha, V. M., M. J. Matthewson, C. R. Kurkjian, K. C. Yoon, J. S. Yoon and C. Y. Moon (2002). Effect of secondary coating on the fatigue and aging of fused silica fibers, *Optical Fiber and Fiber Component Mechanical Reliability and Testing Ii*, Vol. 4639, pp. 75-81, ISSN: 0277-786X.

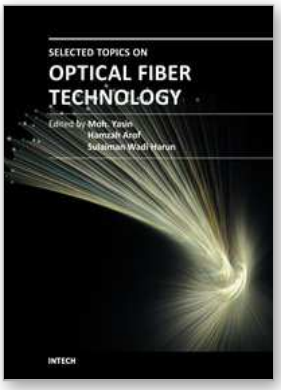

Selected Topics on Optical Fiber Technology

Edited by Dr Moh. Yasin

ISBN 978-953-51-0091-1
Hard cover, 668 pages
Publisher InTech
Published online 22, February, 2012
Published in print edition February, 2012

This book presents a comprehensive account of the recent advances and research in optical fiber technology. It covers a broad spectrum of topics in special areas of optical fiber technology. The book highlights the development of fiber lasers, optical fiber applications in medical, imaging, spectroscopy and measurement, new optical fibers and sensors. This is an essential reference for researchers working in optical fiber researches and for industrial users who need to be aware of current developments in fiber lasers, sensors and other optical fiber applications.

How to reference

In order to correctly reference this scholarly work, feel free to copy and paste the following:

Paulo Antunes, Fátima Domingues, Marco Granada and Paulo André (2012). Mechanical Properties of Optical Fibers, Selected Topics on Optical Fiber Technology, Dr Moh. Yasin (Ed.), ISBN: 978-953-51-0091-1, InTech, Available from: http://www.intechopen.com/books/selected-topics-on-optical-fiber-technology/mechanical-properties-of-optical-fibers

INTECH
open science | open minds

InTech Europe
University Campus STeP Ri
Slavka Krautzeka 83/A
51000 Rijeka, Croatia
Phone: +385 (51) 770 447
Fax: +385 (51) 686 166
www.intechopen.com

InTech China
Unit 405, Office Block, Hotel Equatorial Shanghai
No.65, Yan An Road (West), Shanghai, 200040, China
中国上海市延安西路65号上海国际贵都大饭店办公楼405单元
Phone: +86-21-62489820
Fax: +86-21-62489821